Extended X-ray Absorption Fine Structure (EXAFS) Studies of Hydroxo(oxo)iron Aggregates and Minerals, and a Critique of Their Use as Models for Ferritin

Sarah L. Heath, John M. Charnock, C. David Garner and Annie K. Powell*

Abstract: Structural models for the hydroxo(oxo)iron core of ferritin include extended mineral structures and cluster systems such as $[Fe_{11}O_6(OH)_6(O_2CPh)_{15}]$ ($= Fe_{11}$) and two clusters that crystallise in the same lattice (compound **1**), namely, $[Fe_{17}(\mu_3\text{-}O)_4(\mu_3\text{-}OH)_6(\mu_2\text{-}OH)_{10}(heidi)_8(H_2O)_{12}]^{3+}$ and $[Fe_{19}(\mu_3\text{-}O)_6(\mu_3\text{-}OH)_6(\mu_2\text{-}OH)_8(heidi)_{10}(H_2O)_{12}]^{1+}$. The suitability of these systems as models for the structure of the core of ferritin has been tested by comparing their Fe K-edge EXAFS and X-ray crystallographic results with the Fe K-edge EXAFS data on horse spleen ferritin. The interpretative procedure for the EXAFS analysis was optimised by using the X-ray crystallographic data for compound **1** as a basis. This protocol was then used to interpret the Fe K-edge EXAFS spectra of α- and γ-Fe(O)OH and to reinterpret that previously recorded for horse spleen ferritin. The published Fe K-edge EXAFS data on Fe_{11} were also considered. The Fe···Fe distances provide a clear indication of the nature of the hydroxo(oxo)iron assembly. It was found that the iron–iron interactions are the most reliable guide. Clusters are shown to be more appropriate than infinite lattices as structural models for the core of ferritin.

Keywords
biomimetic chemistry · EXAFS spectroscopy · ferritin · iron homeostasis · nanoparticles

Introduction

The protein ferritin plays a vital role in maintaining iron homeostasis in the majority of life forms.[1] This is best understood in mammalian systems where it is known that the protein provides a spherical cavity with a diameter of 70–80 Å for the storage of iron in the form of Fe^{III} oxyhydroxide mineral phases. Although the protein structure has been determined for horse spleen ferritin (HSF)[2] it has not been possible to resolve details of the iron(III) oxyhydroxide core. Understanding might be improved given better methods of monitoring both the chemical and structural nature of the mineral iron deposits. It is also of inherent scientific interest to investigate how cluster shape and size can influence physical properties.[3]

A calculation assuming the cavity of ferritin is filled by a hydroxo(oxo)iron aggregate with a density of 2 $g\,cm^{-3}$ suggests that up to 4500 irons could be accommodated. Experimentally it proves hard to load more than about 2500.[4] This suggests that there is an element of random distribution in operation. This could be an unequal loading of individual ferritin molecules (where ferritin indicates mammalian-derived protein), or it could be a consequence of the way in which ferritin is loaded leading to disorder and inefficient packing of the cavity. Furthermore it is not known whether the iron centres in ferritin form one crystallite or several smaller crystallites. Attempts have been made to relate the core of ferritin to known mineral types.[1] One problem with this arises from the fact that even if the ferritin is fully loaded with 4500 hydroxo(oxo)iron units in the core and all of these are in the same crystallite corresponding to a portion of a hydroxo(oxo)iron mineral, the size limitation of the cavity means that a particle of no more than 8 nm in diameter will form having about 30% of these units lying on the surface of the sphere, with the remaining 70% defining the bulk. Therefore, although the hydroxo(oxo)iron units in the bulk will be in environments corresponding to those of the hydroxo(oxo)iron units in the extended mineral lattice, those at the surface will be subject to very marked boundary effects as a consequence of the small size of the particle. This leads to difficulties in defining the structure of the mineral portion which is trapped within the ferritin molecule. Diffraction experiments on the cores will suffer from the fact that the physical interpretation of X-ray diffraction data requires that the assumption can be made that the lattice under study corresponds to a truly infinite array with no boundaries. Whilst this is reasonable even for very small single crystals of micrometre dimensions, containing very many more hydroxo(oxo)iron units than the ferritin core can accommodate, in which over 99.75% of the molecules would be in the bulk with only about 0.25% on the surface and therefore with no discernible boundary effects, this is patently not the case for ferritin. The fact that ferritin cores exhibit unusual magnetic properties associated with their nanoscale proportions further underlines this. All this means that the structural details of the core would best be found by using single crystal X-ray diffrac-

[*] Dr. A. K. Powell, Dr. S. L. Heath
School of Chemical Sciences, University of East Anglia
Norwich, NR47TJ (UK)
Fax: Int. code +(1603)593-140
e-mail: a.powell@uea.ac.uk
Prof. C. D. Garner, Dr. J. M. Charnock
Department of Chemistry, University of Manchester
Manchester, M139PL (UK)

0947-6539/96/0206-0634 $ 15.00+.25/0

tion data on loaded ferritin as part of a complete protein structure determination. However, because of the problems of achieving uniform iron-loading and the sheer size of the task, requiring the location of the positions of several thousand iron centres, this route is not currently viable.

Models so far suggested for the ferritin core include the mineral ferrihydrite.[5] However, there is some controversy about the exact nature of the iron sites in ferrihydrite,[5–8] and this may in fact be a collection of mineral phases. Better defined mineral structures such as goethite and lepidocrocite should be more useful as models since they are crystallographically well characterised. A problem with these models for the iron core of ferritin is that they *can* be regarded as infinite structures. As noted above, whilst we can think of the ferritin core as containing encapsulated portions of such an infinite crystal lattice or crystal lattices, these are too small to be treated conventionally. A better approach might be to regard the cores as being in the form of a cluster (or several cluster) aggregate(s) of nanoscale proportions bound within the protein's organic boundary giving rise to at least two distinct iron environments in significant proportions: those at the surface, and those in the bulk. Therefore, there is a need for cluster models that reproduce the various iron environments found in ferritin, ideally with the same distribution. Additionally, such chemical systems would increase our understanding of the structural nature of the ferritin core and should lead to insights into the process of biomineralisation. The iron(III) oxyhydroxide mineral phases, which constitute the core, appear to be different from the terrestrial mineral phases usually encountered in that the iron can be easily mobilised: the challenge that iron-dependent Nature has risen to so splendidly since the advent of photosynthesis and the consequent oxidising atmosphere led to the stabilisation of the III oxidation state of iron. This control over mineral structure and function is a goal which materials scientists pursue vigorously.

Clusters where the irons are all in the III oxidation state, include the previously reported $[Fe_{11}O_6(OH)_6(O_2CPh)_{15}]$[9] and two clusters that crystallise in the same lattice of compound **1** synthesised in our laboratory, namely, $[Fe_{17}(\mu_3\text{-}O)_4(\mu_3\text{-}OH)_6(\mu_2\text{-}OH)_{10}(heidi)_8(H_2O)_{12}]^{3+}$ and $[Fe_{19}(\mu_3\text{-}O)_6(\mu_3\text{-}OH)_6(\mu_2\text{-}OH)_8(heidi)_{10}(H_2O)_{12}]^{1+}$.[10, 11] The clusters in **1** have cores that can be regarded as finite "trapped" mineral structures and are likely to provide better models for the ferritin core than infinite mineral systems. In particular they contain significant proportions of iron atoms in different environments, as is thought to be the case in ferritin. In view of their relevance to the manner in which iron(III) is stored in ferritin, they can be used to calibrate techniques such as EXAFS, which have been used to probe the structure of the iron core in ferritin.[12–17] Additionally they should be better models for specific properties, such as magnetic behaviour, which will be different in finite, bound systems and infinite systems. In order to test these ideas we have measured and compared the iron K-edge EXAFS spectra for **1**, α-Fe(O)OH (goethite) and γ-Fe(O)OH (lepidocrocite), and these results have further been compared with those previously reported for HSF and $[Fe_{11}O_6(OH)_6(O_2CPh)_{15}]$.

Results and Discussion

Crystallography: The crystal structure of **1** has been described elsewhere.[10, 11] The crystal lattice can be regarded as two interpenetrating sets of Fe17 and Fe19 clusters with their mean planes at an angle of 28.4° with respect to each other. The crystal structure parameters were used for comparison with the EXAFS data, and since the latter can be interpreted in terms of average iron environments and does not include any angular information, the actual crystal packing is irrelevant here.

EXAFS: The Fe K-edge EXAFS spectra of α- and γ-Fe(O)OH and the best-fit simulated spectra at 77 K together with their associated Fourier transforms are presented in Figure 1. The

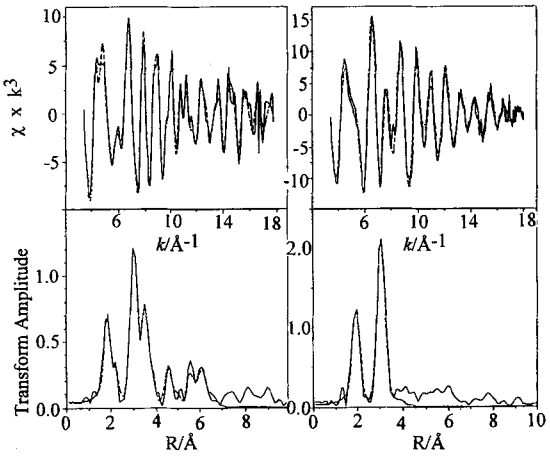

Fig. 1. The EXFAS spectra and fits of α-Fe(O)OH (top left) and γ-Fe(O)OH (top right) and their associated Fourier transforms (bottom left and right, respectively).

best-fit parameters obtained by using phase shifts calculated from **1** are compared with the crystallographic results[18, 19] in Tables 1 and 2. The Fe K-edge EXAFS spectra of **1** and the

Table 1. Comparison of the EXAFS fit (at 77 K) with the crystallographic fit [18] for α-Fe(O)OH (goethite).

Shell	Scatterers	EXAFS R/Å	EXAFS $2\sigma^2$/Å² [a]	Crystallography R(av)/Å	Crystallography R(range)/Å
1	3O	1.95	0.009	1.953	1.953–1.954
2	3O	2.09	0.013	2.090	2.089–2.093
3	2Fe	3.0	0.007	3.010	3.010
4	2Fe	3.28	0.008	3.281	3.281
5	4Fe	3.43	0.008	3.459	3.459
6	10O	3.58	0.004	3.627	3.589–3.916

[a] Debye–Waller parameter.

Table 2. Comparison of the EXAFS fit (at 77 K) with the crystallographic fit [19] for γ-Fe(O)OH (lepidocrocite).

Shell	Scatterers	EXAFS R/Å	EXAFS $2\sigma^2$/Å² [a]	Crystallography R(av)/Å	Crystallography R(range)/Å
1	6O	2.00	0.012	2.041	1.905–2.133
2	6Fe	3.05	0.011	3.076	3.074–3.080
3	6O	3.74	0.033	3.665	3.622–3.687
4	2Fe	3.94	0.008	3.870	3.870

[a] Debye–Waller parameter.

best-fit simulated spectra at 300 and 77 K together with their associated Fourier transforms are presented in Figure 2. The best-fit parameters are compared with the crystallographic results in Table 3.

The EXAFS spectrum is an average of contributions from all of the iron atoms. A loss of information about the specific iron environments occurs, particularly for the outer shells where the different environments of the iron atoms tend to smear out fine

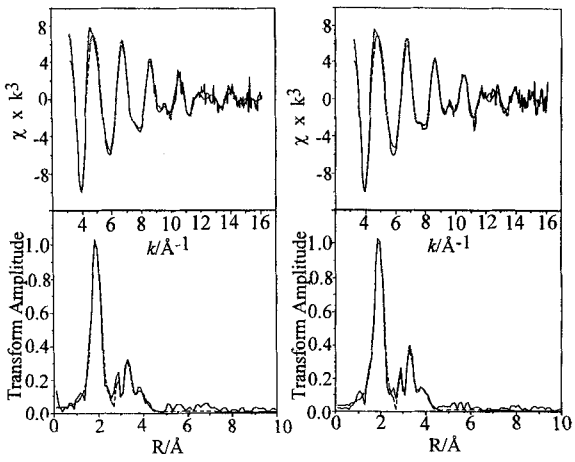

Fig. 2. The EXAFS and best-fit simulated spectra of **1** at 77 (top left) and 300 K (top right) with their associated Fourier transforms (bottom left and right, respectively).

details. In order to get a good simulation of the Fe K-edge EXAFS of **1** it was necessary to include five shells of backscatterers. The first shell is interpreted as a shell of six oxygen atoms at 1.97 Å corresponding to the primary coordination sphere. This is in reasonably good agreement with the crystal structure determination of **1** where the average Fe–O/N distance is 2.022 Å.[11] The average Fe–O bond length in **1** is 2.005 Å; the iron atoms around the periphery are coordinated by four oxygen atoms and one nitrogen atom from the ligand heidi ($N(CH_2CO_2^-)_2(CH_2CH_2O^-)$) and one oxygen atom from a coordinated water molecule. The lower affinity of iron for nitrogen means that the average Fe–N bond length (2.216 Å) is some 10% longer than the average Fe–O lengths (2.005 Å) in **1**. As can be seen from Tables 3 and 4 the iron–light atom lengths cover a considerable range with the shortest of 1.834 Å observed for Fe coordinated to μ_3-oxide and the longest of 2.253 Å for Fe coordinated to nitrogen. When attempting to fit a single shell of backscatterers to such a wide range of distances, the EXAFS value tends to be lower than the actual average distance.[20]

Table 3. Comparison of the EXAFS fit with the crystallographic fit of **1**.

		EXAFS				Crystallography	
		300 K		77 K			
Shell	Scatterers	R/Å	$2\sigma^2$/Å^2 [a]	R/Å	$2\sigma^2$/Å^2 [a]	R(av)/Å	R(range)/Å
1	6 O [b]	1.97	0.018	1.97	0.018	2.022[b]	1.834–2.253
2	0.33 Fe	2.91	0.006	2.93	0.004	2.967	2.948–2.999
3	1.33 Fe	3.15	0.022	3.15	0.018	3.160	3.104–3.219
4	2.33 Fe	3.51	0.029	3.51	0.023	3.501	3.386–3.629
5	8 O	3.56	0.035	3.56	0.034		

[a] Debye–Waller parameter. [b] Treating the nitrogens coordinated to the peripheral iron atoms as oxygen.

Table 4. Details of iron environments for **1**.

Bond type	Average Fe_{19}/Å	Average Fe_{17}/Å
Fe–N	2.220(28)	2.210(37)
Fe–O (water)	2.118(23)	2.082(29)
Fe–μ_2-OH	1.950(20)	1.952(22)
Fe–O (carboxylate)	1.995(23)	1.979(28)
Fe–μ_3-O	1.934(19)	1.930(22)
Fe–μ_3-OH	2.091(18)	2.079(21)
Fe–O (alkoxide)	1.989(21)	1.993(25)

Attempts were made to simulate the spectra by taking account of all the different Fe–O and Fe–N distances as detailed in Table 4, but this did not produce a significantly better fit and, in view of the dangers of overparameterisation, it was decided to proceed with the analysis based on a single primary coordination sphere. Thus, metal edge EXAFS cannot really be used to provide this sort of fine detail for such a complicated system, even when the exact structural parameters are known. In addition, the backscattering amplitude and the phase shift of the nitrogen and oxygen are very similar and these atoms cannot be safely distinguished in the EXAFS analysis. Thus, all the backscattering contributions from light atoms were included as oxygens. Three shells of iron backscatterers are necessary to fit the features in the EXAFS that give rise to peaks between 2.5 and 3.8 Å in the Fourier transform. Inclusion of a further shell of light atoms at 3.5 Å significantly improves the fit in the low k region of the spectrum; these atoms could arise from the oxygens or carbons of the heidi ligands around the peripheral irons as can be calculated from the crystal structure analysis. Such effects at the boundary of the cluster could also be important in ferritin, as pointed out previously[15] where it was also necessary to include a shell of low atomic number backscatterers at 3.6 Å in order to improve the simulation of the low k region.

To fit the EXAFS data of the models, the numbers of backscatterers in each shell (N) were fixed at the crystallographic values. When allowed to float, the numbers of iron backscatterers in α-Fe(O)OH at 3.02, 3.29 and 3.44 Å became 1.9, 2.0 and 4.0, respectively, in good agreement with the crystallographic values of 2, 2 and 4. However, in γ-Fe(O)OH, N for the shell at 3.07 Å became 4.6, significantly lower than the expected value of 6. In the analysis of compound **1**, the values of N for the iron shells at 2.93, 3.15 and 3.51 Å became 0.5, 1.7 and 0.9, respectively, compared with the crystallographic averages of 0.33, 1.33 and 2.33. These results demonstrate that EXAFS cannot be used to give reliable values of the numbers of atoms in outer shells, especially in situations in which the central atom is present in a variety of different sites. Despite this, it is manifest that EXAFS does give useful information about the average environment of iron atoms, in particular Fe···Fe distances, even in large clusters. The overall pattern observed, with three different shells of iron atoms necessary to fit the data, clearly shows that even in this system with 36 iron atoms in the unit cell in 19 different sites it is possible to use EXAFS to resolve contributions from different types of Fe···Fe separation. Such distances are diagnostic of the number of bridging atoms, that is, of vertex, edge or face sharing of coordination polyhedra.[21] For example, in compound **1**, for a given linkage the Fe···Fe separation can be affected by the chemical nature of the bridging atom(s). Thus the most useful approach to looking at the EXAFS of ferritin and its models is to consider the interpretation of the Fe···Fe interactions.

Comparison with ferritin and other models for ferritin: As described elsewhere[10,11,22] the structures of the Fe_{17} and Fe_{19} clusters (Figs. 3 and 4) both comprise an inner hexagonal close-packed (hcp) iron(III) hydroxide core, related to the brucite ($Mg(OH)_2$) structure, which is enclosed by a layer of iron nucleation sites attached to the inner surface of a shell of organic ligands. The cores correspond to trapped portions of the mineral phase, $\{Fe(OH)_2^+\}_\infty$, which cannot exist under normal conditions, and it is the charge compensation of the shell by heidi that allows this to be stabilised. In this way the ligand heidi has the effect of dictating mineral structure, dimensionality and charge. The three iron shells derived from the EXAFS data correspond to three distinguishable groups of Fe···Fe distances seen in the

0947-6539/96/0206-0636 $ 15.00+.25/0 Chem. Eur. J. 1996, 2, No. 6

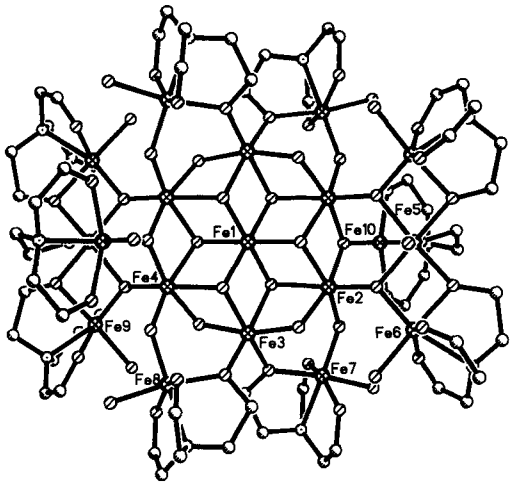

Fig. 3. The molecular structure of $[Fe_{19}(\mu_3\text{-}O)_6(\mu_3\text{-}OH)_6(\mu_2\text{-}OH)_8(heidi)_{10}(H_2O)_{12}]^+$.

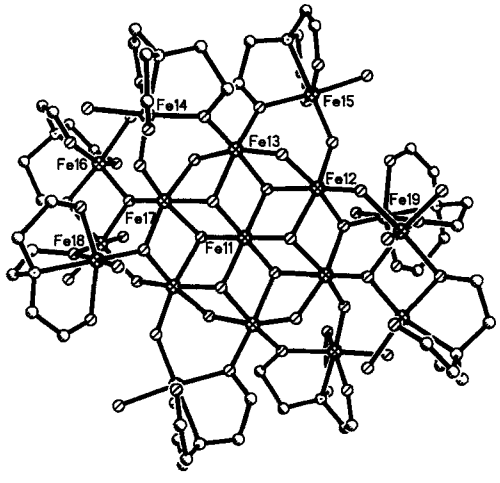

Fig. 4. The molecular structure of $[Fe_{17}(\mu_3\text{-}O)_4(\mu_3\text{-}OH)_6(\mu_2\text{-}OH)_{10}(heidi)_8(H_2O)_{12}]^{3+}$.

crystal structure. These have direct parallels with the situation in ferritin as illustrated in Figure 5. They are:

a) The interactions between the iron atoms in the core.
b) The interactions between iron atoms in the core with iron atoms in the surrounding nucleation shell.
c) The interactions between iron atoms in the nucleation shell.

The shortest Fe···Fe distances in **1** identified by EXAFS is a shell of 0.33 iron atoms[23] at 2.93 Å this corresponds to the short Fe···Fe distances between Fe5 and Fe9a (symmetry equivalent of Fe9), Fe5 and Fe6, Fe16 and Fe18 and their symmetry equivalent atoms (Figs. 3 and 4), that is, to c-type interactions between pairs of irons in the nucleation shell. These groups are characterised by two bridging oxygen atoms, one from a heidi ligand and the other from a μ_3-oxo group. This has the consequence of holding the pairs of iron atoms close together, and the average crystallographic distance between these irons is 2.976 Å, ranging from 2.948 to 2.999 Å. The next shell of iron backscatterers in compound **1** identified by EXAFS comprises 1.33 iron atoms[23] at 3.15 Å. This corresponds to the pairs of iron atoms such as Fe1 and Fe2, that is, to a-type interactions between pairs of iron atoms in the core. These are principally bridged by μ_2- and μ_3-hydroxo groups, with average crystallographic distances of 3.160 Å (in the range 3.104–3.219 Å). The final shell of iron backscatterers identified by EXAFS comprises 2.33 iron atoms[23] at 3.51 Å, due to pairs of iron atoms such as Fe2 and Fe5 (corresponding to b-type interactions between iron atoms in the core and the nucleation shell). These atoms are bridged by a μ_3-oxo atom and their crystallographic separation is an average of 3.501 Å and ranges from 3.386 to 3.629 Å.[24]

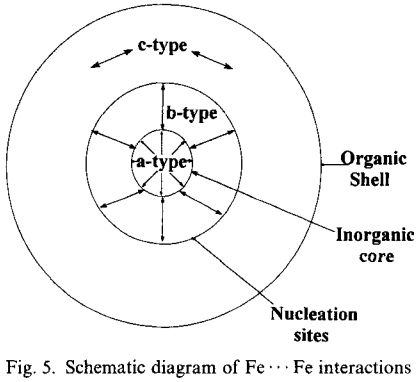

Fig. 5. Schematic diagram of Fe···Fe interactions in **1**.

The EXAFS study of **1** provides insights into modelling the cores of the iron-storage proteins such as ferritin. For example, analysis of the EXAFS spectrum of HSF (see Table 5) described herein shows that in the core the average iron environment is six oxygen atoms at 1.96 ± 0.03 Å (cf. the earlier value of 1.93 Å[15]), with a split shell of iron atoms at 3.01 and 3.43 Å (cf. the earlier values of 2.95 and 3.39 Å[15]). There is also evidence for a shell of oxygens at 3.54 Å (cf. the earlier value of 3.59 Å[15]) and for a shell of oxygens or other light scatterers in **1** at 3.56 Å (see Table 1), mirroring the situation in ferritin. The results of the EXAFS studies on **1** suggest that the split iron shell in ferritin could arise from a combination of a- and c-type interactions (average = 3.1 Å) with b-type interactions (average = 3.5 Å).

The above analysis indicates that **1** provides a good model for ferritin, both in terms of its EXAFS data and structure. This is reinforced by Figure 6, which shows a comparison of the Fe K-edge EXAFS of ferritin and compound **1** together with their Fourier transforms. The latter show clearly the correspondence of the radial distribution curves; the Fe···Fe separations are more clearly resolved in **1** than in ferritin, as might have been anticipated from the relative sizes of the aggregates. Thus the broad asymmetric envelope for HSF with its maximum at approximately 3.1 Å includes the three distinct peaks (2.93, 3.13 and 3.51 Å) for compound **1**. It should also be noted that the

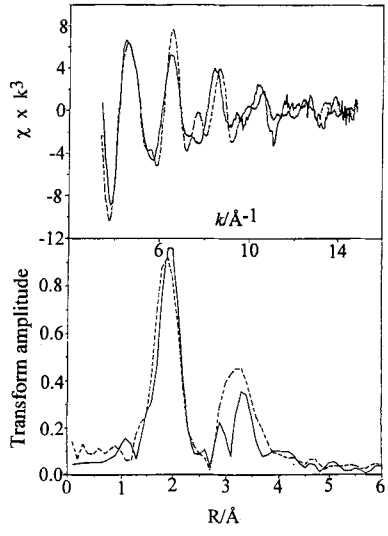

Fig. 6. The comparison of the EXAFS spectra (top) with their Fourier transforms (bottom) for HSF (dotted line) and compound **1** (solid line).

Table 5. Comparison of the EXAFS for HSF, **1**, Fe_{11} [14], α-Fe(O)OH and γ-Fe(O)OH (values in brackets are given where two shells have been combined to aid comparison).

Sample	Shell 1 Scatterers	Shell 1 R(av)/Å	Shell 2 Scatterers	Shell 2 R(av)/Å	Shell 3 Scatterers	Shell 3 R/Å	Shell 4 Scatterers	Shell 4 R/Å
HSF [a]	6O	1.96	1.5 Fe	3.01	1.1 Fe	3.43	8O	3.54
1 [b]	6O	1.97	1.33 Fe (1.66 Fe) 0.33 Fe	3.15 (3.11) 2.93	2.33 Fe	3.51	8O	3.56
Fe11	6O	1.96	2.2 Fe	3.00	2.80 Fe	3.48	[e]	
α-Fe(O)OH [c]	3O (6O) 3O	1.95 (2.02) 2.09	2 Fe (4 Fe) 2 Fe	3.02 (3.16) 3.29	4 Fe	3.44	10O	3.58
γ-Fe(O)OH [d]	6O	2.00	6 Fe	3.07	–	–	6O	3.74

[a] $E0$ = 24.7 for the O and 26.3 for the Fe backscatterers. [b] $E0$ = 25.7 for the O and 27.2 for the Fe backscatterers. [c] $E0$ = 21.7 for the O and 23.2 for the Fe backscatterers. [d] $E0$ = 22.1 for the O and 23.5 for the Fe backscatterers. [e] No data available.

relative size of the corresponding peaks in the Fourier transforms of α- and γ-Fe(O)OH are much larger.

The Fe K-edge EXAFS data for other possible models of the ferritin core whose crystal structures are also known are presented together with the EXAFS interpretation of **1** in Table 5 given in order of decreasing correspondence to the interpretation of the ferritin EXAFS. The molecular species **1** and Fe_{11} have 3.99 and 5.0 Fe's, respectively, within 3.6 Å, as compared with 2.6 for ferritin, and these can be divided into two shells. For the mineral models, α-Fe(O)OH (Fig. 7) has 8 Fe's within 3.6 Å, which can

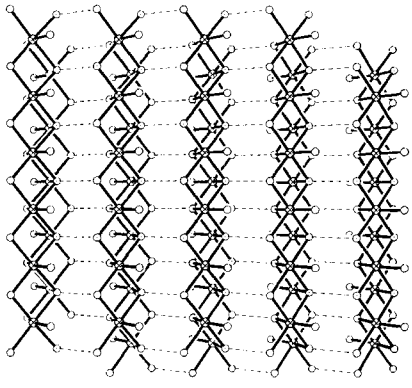

Fig. 7. The crystal structure of goethite, α-Fe(O)OH.

be divided into three shells, although we have combined the first two into one shell (shell 2) in Table 5 to aid comparison. γ-Fe(O)OH (Fig. 8) has 6 Fe's within 3.6 Å, and these are all in one shell, which is at 3.07 Å. As noted above the occupation numbers from EXAFS can only reliably be used as a qualitative guide rather than quantitative figures and, as such, indicate that

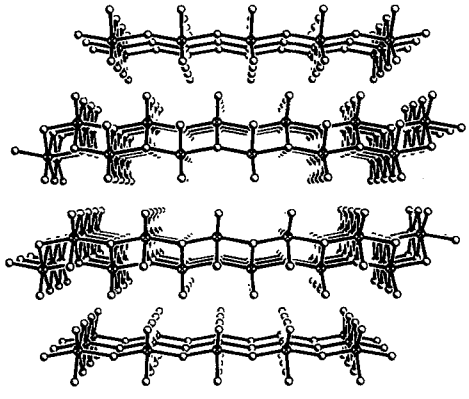

Fig. 8. The crystal structure of lepidocrocite, γ-Fe(O)OH.

a cluster such as **1** provides data closer to that of ferritin than the mineral models.

Although their interpretation of the EXAFS data on the Fe_{11} complex fits quite well with our interpretation of the EXAFS on ferritin,[15] Islam et al. interpreted the EXAFS somewhat differently and concluded that their complex was not a good model for ferritin,[14] but rather for an intermediate in the formation of ferritin cores. Their approach did not involve using the crystallographically characterised complex to calibrate the phase shifts of the EXAFS data as we have done here. Although the complex Fe_{11} is an encapsulated cluster it does not have a close-packed core and is not related to any mineral form. As such it does not realistically model the currently accepted situation in ferritin.[25] A comparison of the data for the two infinite mineral models, the α and γ forms of Fe(O)OH, illustrates the effect that hexagonal versus cubic close-packing of the anions has on the local environments of the irons. As can be seen in Table 3 and is to be expected in view of the fact that both contain hcp structures, the EXAFS of α-Fe(O)OH rather than γ-Fe(O)OH is more like that of **1**. As mentioned above, **1** contains hcp cores of the brucite structure, and the relationship of the layer structure of AX_2 hydroxides to those containing μ_4-oxo bridges found in the series of hydroxo(oxo)-M^{III} clusters has been pointed out previously.[10, 22, 26] The crystallographic data on oxides such as α-Fe_2O_3 (haematite) show that they are clearly inappropriate for modelling the EXAFS of ferritin, since they possess even closer Fe···Fe interactions than the other two mineral models analysed here. In the case of haematite there are 7 Fe's within 3.4 Å and 7 more at less than 4 Å.[27]

Compound **1** gives the best correspondence to the Fe K-edge EXAFS of ferritin because it reproduces the major structural features of ferritin. The other cluster model, Fe_{11}, does not possess all these features, and therefore the fit is not quite as good, although it is much better than that of the mineral models. Although α-Fe(O)OH is a more convincing model than γ-Fe(O)OH, neither of the minerals examined here produce Fe K-edge EXAFS data much like that of ferritin; too many shells of iron atoms are within 3.6 Å of an iron atom. This leads to the suggestion that the core of ferritin contains predominantly hcp hydroxo(oxo)irons. A further point is that the proportion of iron found in fully loaded ferritin is between 25 and 30%. Compound **1** contains 27% iron, Fe_{11} 23% and Fe(O)OH 63%, that is, **1** also accurately models the amount of iron found in ferritin.

Conclusions

Of all the well-characterised models for the ferritin core, it is clear that the cluster compounds give EXAFS spectra that better fit that of ferritin than do those of infinite crystal structures.

0947-6539/96/0206-0638 $ 15.00+.25/0 Chem. Eur. J. 1996, 2, No. 6

This is to be expected, since clusters possess many different iron environments just as ferritin does. We have shown that the best approach is to interpret the EXAFS in terms of the Fe···Fe interactions, since the fine detail of the immediate coordination sphere can be lost. This implies that it might not be possible to identify a small number ($\leq 5\%$) of tetrahedral iron sites in a structure where the sites are predominantly octahedral, as has been proposed by other groups working in the area of mineral ferrihydrite.[5] However, there is much debate on the likely structure of the mineral ferrihydrite, and it seems possible that it is actually a collection of phases, most of which are not particularly crystalline, and therefore it will not be possible to determine a definitive structure.

In HSF there is an outer coat of organic ligands from the protein. Iron(III) ions interact with the amino acid residues on the inside of this coat to form nucleation sites. Further iron(III) ions then complex to these through oxo and hydroxo bridges. More iron(III) ions building on to these in a similar fashion would result in the growth of a single crystallite of a hydroxo-(oxo)iron(III) core.[28] Therefore good cluster models for ferritin should exhibit three main features: close-packed cores, inner nucleation sites and an organic coat. It is clear that clusters such as **1** model this situation closely in that they consist of an inorganic mineral core connected to an encapsulating organic shell through iron/ligand "nucleation" sites on the inner surface of this shell.

It is conceivable that the biomineral cores of proteins such as ferritin possess different structural types from those normally encountered for iron(III) minerals, as is the case with **1**. This could be a direct result of the stereochemical demands imposed by the nucleation sites on the protein shell. It is only by producing increasingly better models for ferritin that we can resolve this question.

Experimental Procedure

Compound **1**, HSF and the hydroxo(oxo)iron minerals were prepared as described previously [11,13,15]. The samples of **1** and α- and γ-Fe(O)OH were prepared for X-ray absorption spectroscopic investigation by grinding ca. 0.2 g of the material with an equal amount of boron nitride, and the resulting powder was contained in a thin aluminium sample holder with sellotape windows. The X-ray absorption spectra were measured in transmission mode at the Fe K-edge on station 7.1 at the Daresbury Synchrotron Radiation Source, operating at 2 GeV with an average current of 150 mA for the sample maintained at 300 and at 77 K. For the latter the samples were mounted on the cold finger of a cryostat cooled by liquid nitrogen in an evacuated sample chamber with thin Mylar windows. A Si(111) double-crystal monochromator was used, with the second crystal offset to give 50% rejection of the beam in order to remove harmonic contamination. One scan was taken at each temperature. After background subtraction the EXAFS was analysed using the curved wave theory [29,30] in the Daresbury program EXCURV92 [31]. Phase shifts were calculated ab initio in the program with Xα ground state and potentials using the default values for muffin tin radii, and exchange potentials and the parameters AFAC and VPI were set at 0.70 and −1, respectively. The value of E_0 was allowed to float to give the optimum fit for the EXAFS data at 77 K and kept fixed at the same value in the analysis of the EXAFS data at ambient temperature. The EXAFS were simulated by building up a model using parameters derived from the crystal structures and then allowing the shell distances and the Debye–Waller factors A ($= 2\sigma^2$) to vary until the best fit to the experimental EXAFS spectrum was found. The Joyner statistical test [32] was used on the addition of each shell beyond the first in order to check the significance of any improvement in the fit. Only shells with a statistical significance at the 1% level were included in the final fit. The initial analysis of the spectrum of **1** showed the Fe···Fe distances to be slightly shorter than the crystallographic values; a correction factor was therefore applied to E_0 for the shells of the iron backscatterers, which was allowed to float to give the optimum fit. This naturally improved the fit between the experimental and calculated EXAFS and also gave a better agreement with the crystallographic data. This protocol was used to reanalyse the Fe K-edge EXAFS for α- and γ-Fe(O)OH and HSF [15]. The results of these analyses, that for compound **1** and that reported by others for Fe_{11} [14] are compared in Table 5. The protocol now employed led to some small changes to the shell distances previously published for HSF [15]. For the latter we found slightly longer Fe···Fe distances than in the original analysis, but no significant change to the published interpretation. Thus the overall approach was to use a crystallographically characterised model (**1**) as a means of testing and refining the interpretative procedure for EXAFS analysis of HSF, α- and γ-Fe(O)OH. Since the raw data on Fe_{11} were not available no reanalysis of the Fe K-edge EXAFS was performed.

Acknowledgements: We would like to thank the SERC for the provision of a grant and the CDS data bank at Daresbury and Daresbury Laboratory for the provision of beamtime.

Received: August 21, 1995 [F192]

[1] R. R. Crichton, *Inorganic Biochemistry of Iron Metabolism*, Horwood, New York, **1991**.
[2] G. C. Ford, P. M. Harrison, D. W. Rice, J. M. A. Smith, A. Treffrey, J. L. White, J. Yariv, *Philos. Trans. R. Soc. London* **1984**, *B304*, 551–565.
[3] G. Schmid, *Clusters and Colloids: From Theory to Application*, VCH, Weinheim, **1994**.
[4] A. Trefry, P. M. Harrison, *J. Biochem.* **1979**, *181*, 709–716
[5] R. A. Eggleton, R. W. Fitzpatrick, *Clays Clay Miner.* **1988**, *36*, 111–124.
[6] K. M. Towe, W. F. Bradley, *J. Colloid Interface Sci.* **1967**, *24*, 384–392.
[7] A. Manceau, J. M. Combes, G. Calas, *Clays Clay Miner.* **1990**, *38*, 331–334.
[8] R. A. Eggleton, R. W. Fitzpatrick, *Clays Clay Miner.* **1990**, *38*, 335–336.
[9] S. M. Gorun, G. C. Papaefthymiou, R. B. Frankel, S. J. Lippard, *J. Am. Chem. Soc.* **1987**, *104*, 3337.
[10] S. L. Heath, A. K. Powell, *Angew. Chem.* **1992**, *104*, 191–192; *Angew. Chem. Int. Ed. Engl.* **1992**, *31*, 191–193.
[11] A. K. Powell, S. L. Heath, D. Gatteschi, L. Pardi, R. Sessoli, G. Spina, F. Del Giallo, F. Pieralli, *J. Am. Chem. Soc.* **1995**, *117*, 2491–2502.
[12] E. C. Theil, D. E. Sayers, M. A. Brown, *J. Biol. Chem.* **1979**, *254*, 8132–8134.
[13] P. Mackle, PhD Thesis, University of Manchester **1991**.
[14] Q. T. Islam, D. E. Sayers, S. M. Gorun, E. C. Theil, *J. Inorg. Biochem.* **1989**, *36*, 51.
[15] P. Mackle, C. D. Garner, R. J. Ward, T. J. Peters, *Biochim. Biophys. Acta* **1991**, *1115*, 145.
[16] S. M. Heald, E. A. Stern, B. Bunker, E. M. Holt, S. L. Holt, *J. Am. Chem. Soc.* **1979**, *101*, 76–73.
[17] J. S. Rohrer, T. I. Quazi, G. D. Watt, E. D. Sayers, E. C. Theil, *Biochemistry* **1990**, *29*, 259–264.
[18] A. Szytula, A. Burewicz, Z. Dimitrijewic, S. Krasnicki, H. Rzany, J. Todorovic, A. Wanic, W. Wolski, *Phys. Status Solidi* **1968**, 429.
[19] H. Christensen, A. N. Christensen, *Acta Chem. Scand. Ser. A* **1978**, *87*, 32.
[20] G. E. Brown, Jr., W. A. Waychunas, C. W. Ponader, W. E. Jackson, D. A. McKeown, *J. Phys. (Paris)* **1986**, *47*, C8-661–C8-668.
[21] A. Manceau, J. M. Combes, *Phys. Chem. Minerals* **1988**, *15*, 283.
[22] A. K. Powell, S. L. Heath, *Comments Inorg. Chem.* **1994**, *15*, 255–296.
[23] In the analysis of the Fe K-edge EXAFS of **1**, the occupation numbers of the shells were fixed at the average value determined by the crystallographic analyses described in references [11] and [12].
[24] A complete tabulation of the Fe···Fe distances is available from the authors as supplementary material.
[25] T. G. St Pierre, J. Webb, S. Mann in *Biomineralisation* (Eds: S. Mann, J. Webb, R. J. P. Williams), VCH, Weinheim, **1989**, 295–344.
[26] K. L. Taft, G. C. Papaefthymiou, S. J. Lippard, *J. Am. Chem. Soc.* **1994**, *33*, 1510–1520.
[27] R. L. Blake, R. E. Hessevick, T. Zoltai, L. W. Finger, *American Mineralogist* **1966**, *51*, 123.
[28] P. M. Harrison, G. A. Clegg, K. May, *Prog. Biophys. Mol. Biol.* **1980**, *36*, 131.
[29] P. A. Lee, J. B. Pendry, *Phys. Rev.* **1975**, *B11*, 2795.
[30] S. J. Gurman, N. Binsted, I. Ross, *J. Phys. C.* **1984**, *17*, 143.
[31] N. Binsted, J. W. Cambell, S. J. Gurman, P. C. Stephenson, SERC Daresbury Laboratory EXCURV92 Program, 1991.
[32] R. W. Joyner, K. J. Martin, P. Meehan, *J. Phys. C.* **1987**, *20*, 4005.